AMERICAN SOCIETY FOR MICROBIOLOGY | Antimicrobial Agents and Chemotherapy®

PHARMACOLOGY

Influence of Experimental Cryptococcal Meningitis in Wistar Rats on Voriconazole Brain Penetration Assessed by Microdialysis

Izabel Almeida Alves,[a] Keli Jaqueline Staudt,[b] Carolina de Miranda Silva,[a] Graziela de Araujo Lock,[a] Teresa Dalla Costa,[a] Bibiana Verlindo de Araujo[a,b]

Pharmaceutical Sciences Graduate Program of Federal University of Rio Grande do Sul, Porto Alegre, Rio Grande do Sul, Brazil[a]; Medical Sciences Graduate Program of Federal University of Rio Grande do Sul, Porto Alegre, Rio Grande do Sul, Brazil[b]

ABSTRACT To make advances in the treatment of cryptococcal meningitis, it is crucial to know a given drug's free fraction that reaches the biophase. In the present study, we applied microdialysis (μD) as a tool to determine the free levels reached by voriconazole (VRC) in the brains of healthy and *Cryptococcus neoformans*-infected rats. The infection was induced by the intravenous (i.v.) administration of 1×10^5 CFU of yeast. The dose administered was 5 mg/kg (of body weight) of VRC, given i.v. Plasma and microdialysate samples were analyzed by liquid chromatography-tandem mass spectrometry (LC-MS/MS) and LC-UV methods. The free brain/free plasma ratio (*f*T) and population pharmacokinetic (popPK) analyses were performed to evaluate the impact of infection on PK parameters of the drug. The brain penetration ratio showed an increase on brain exposure in infected animals ($fT_{healthy} = 0.85$ versus $fT_{infected} = 1.86$). The structural PK model with two compartments and Michaelis-Menten (MM) elimination describes the VRC concentration-time profile in plasma and tissue simultaneously. The covariate infection was included in volume of distribution in the peripheral compartment in healthy animals (V_2) and maximum rate of metabolism (V_M). The levels reached in infected tissues were higher than the values described for MIC of VRC for *Cryptococccus neoformans* (0.03 to 0.5 μg ml^{-1}), indicating its great potential to treat meningitis associated with *C. neoformans*.

KEYWORDS *Cryptococcus neoformans*, voriconazole, microdialysis, population pharmacokinetics analysis, meningitis

Received 13 February 2017 **Returned for modification** 20 March 2017 **Accepted** 28 April 2017

Accepted manuscript posted online 8 May 2017

Citation Alves IA, Staudt KJ, Silva CDM, Lock GDA, Dalla Costa T, de Araujo BV. 2017. Influence of experimental cryptococcal meningitis in Wistar rats on voriconazole brain penetration assessed by microdialysis. Antimicrob Agents Chemother 61:e00321-17. https://doi.org/10.1128/AAC.00321-17.

Address correspondence to Bibiana Verlindo de Araujo, bibiana.araujo@ufrgs.br.

Invasive cryptococcosis is a severe illness which has a high mortality rate (50 to 90%); unfortunately, the effectiveness of initial empirical treatment is directly linked to patient outcome. Despite its universally recognized toxicity, amphotericin B was considered to be the cornerstone for successful therapy in cryptococcal meningitis (1). The less toxic agent fluconazole (FCZ) offered an attractive alternative in the treatment of cryptococcosis and a variety of other invasive fungal infections in nonneutropenic patients (2, 3); however, its use is limited due to resistance of *Cryptococcus* spp. (4). Recently, voriconazole (VRC), which exhibits fungistatic activity against resistant strains of *Cryptococcus* (5, 6), has been recognized as a novel therapeutic option for the treatment of cryptococcal meningitis (7–10), but there are scarce studies focusing on its pharmacokinetic/pharmacodynamic (PK/PD) behavior during the infectious process in the brain.

VRC shows some differences from FCZ, such as its high lipophilicity (log P of 1.83 versus log P of 0.58) (2, 11) and lack of involvement with efflux transporters (12–14) that can aid the drug's distribution in tissues like the brain, suggesting a better distribution

of VRC. Studies comparing the levels reached by these drugs in cerebrospinal fluid (CSF) of patients demonstrated similar levels (0.5 to 0.9 for FCZ versus 0.2 to 1 for VRC) (15), but this technique presents limitations associated with differences between the blood-brain barrier and the blood-cerebrospinal fluid barrier (16, 17).

In order to determine free interstitial concentrations, the "gold standard" method is microdialysis (μD), which has found applications in PK studies, especially in the investigation of drug penetration in various tissues and organs of animals and humans (18). Studies using μD have demonstrated that antimicrobials may show differences between free plasma and free tissue concentrations when drug efflux and influx transporters contribute to distribution (19, 20). Moreover, pathological conditions can change tissue-blood relationships, and antimicrobial concentrations in infected tissues may differ from those in healthy tissues due to increased temperature, decreased pH, plasma extravasations, and leukocyte migration at the infection site (18, 21).

Aiming at a better evaluation of the potential use of voriconazole in the treatment of cryptococcal meningitis, the present study investigated the free interstitial levels reached in the brain by VRC in healthy and *Cryptococcus neoformans*-infected Wistar rats using μD in a population pharmacokinetics (popPK) approach.

RESULTS

Microdialysis. No differences between dialysis and retrodialysis recovery dependency on VRC concentration were observed during *in vitro* CMA 12 probe calibration (data not shown). The best recovery flow *in vitro* was 2.0 μl/min, showing a relative recovery (RR) by dialysis of 24.49% $\pm$ 2.46% and by retrodialysis of 26.13% $\pm$ 2.87% ($P > 0.05$), indicating that VRC does not bind to the μD tubing and the retrodialysis method can be used to determine the recovery *in vivo*.

The RRs determined *in vivo* were 16.35% $\pm$ 4.43% in healthy and 14.91% $\pm$ 3.83% in infected brains. No difference in RRs *in vivo* between healthy and infected animals was observed ($P > 0.05$). In general, the recoveries determined *in vivo* are lower than those determined *in vitro* due to biological characteristics of the tissues where the probes are inserted, such as tortuosity, interstitial fluid volume, drug uptake into cells, the active transport across membranes, the extent of tissue vascularization, and blood flow through the tissue, which can limit the diffusion of the drug through the probes (22). Our group observed an *in vivo* RR of VRC in renal tissue of 25.1% $\pm$ 2.8% in the same flow (2 μl/min) using a CMA 20 (22), and this slight difference can be explained by the type of probe and tissue investigated.

Infection. The yeast count in the brain showed the presence of viable *C. neorformans* in the tissue (6.8 $\pm$ 0.5 $\log_{10}$ CFU/ml), and the histopathological analysis showed yeast elements distributed in clusters similar to cysts (pseudocysts) (23).

Pharmacokinetic analysis. The levels of protein binding of VRC to plasma in rats (pb_{plasma}) were found to be 65% $\pm$ 2.5% for healthy animals and 64% $\pm$ 1.3% for infected animals ($P < 0.05$). These results are similar to those obtained by de Araújo et al. (22) for healthy Wistar rats (66% $\pm$ 4%). No concentration dependence on VRC pb_{plasma} in the range investigated (0.075 to 0.8 μg/ml) was seen. The unbound drug fraction ($1 - p_b$) in plasma was considered for the estimate of drug's fraction in tissue (*f*T) by correcting the total area under the curve (*f*AUC).

The AUC values determined by trapezoidal rule for plasma and tissue in healthy and infected animals were 20.52 $\pm$ 8.45 μg $\cdot$ h/ml, 5.69 $\pm$ 1.51 μg $\cdot$ h/ml, 24.71 $\pm$ 7.54 μg $\cdot$ h/ml, and 13.80 $\pm$ 1.53 μg $\cdot$ h/ml, respectively. Statistic differences between healthy and infected animals ($P < 0.001$) were obtained by Student's *t* test only for the $fAUC_{tissue}$ values. These differences reflect changes in brain penetration between healthy and infected animals, better demonstrated by the comparison of *f*Ts, which were 0.85 $\pm$ 0.22 for healthy and 1.86 $\pm$ 1.05 for infected rats ($P < 0.05$), i.e., an increased brain penetration of 118% in the infected group.

The mean total plasma and free brain concentration-time profiles after VRC intravenous (i.v.) bolus dosing of 5 mg/kg are shown in Fig. 1.

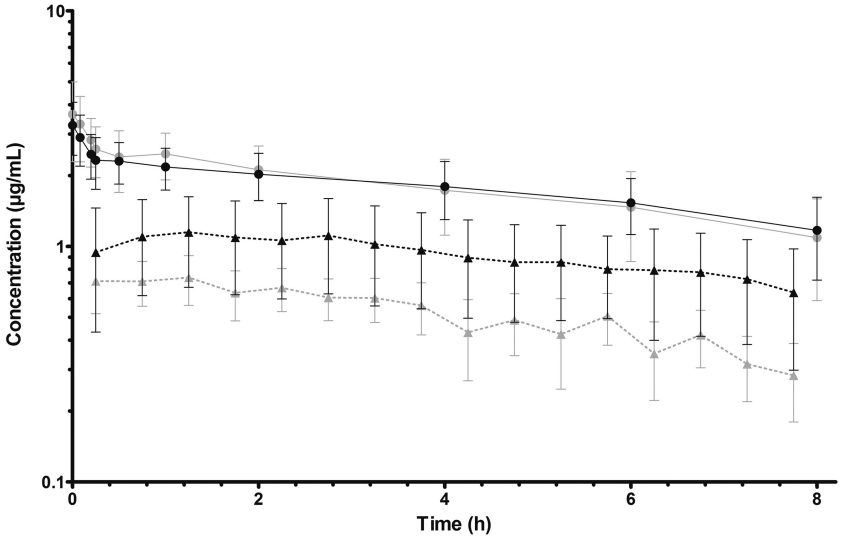

FIG 1 Mean and SD for total plasma from healthy rats (gray dots) and *Cryptococcus neoformans*-infected rats (black dots) and free brain profiles from healthy rats (gray triangles) and *Cryptococcus neoformans*-infected rats (black triangles) after administration of 5 mg/kg of VCZ as an i.v. bolus ($n = 7$ and $n = 5$ for healthy and infected groups, respectively).

Several structural models were proposed to characterize the PK of VRC, including one-, two-, and three-compartment models and linear and nonlinear distribution processes (24, 25). A two-compartment model with Michaelis-Menten (MM) elimination and a combined residual error models for both total plasma and free brain concentrations was selected as the final model. The parameter value k_M (MM constant) was set at 0.54 μg/ml from our previous study in rats for the same dose (25). The system of differential equations for the final model is given in equations 1 to 4.

$$\frac{dA_1}{dt} = k_{21} \times A_2 - \left(k_{12} + \left[\frac{V_M}{k_M + A_1}\right]\right) \times A_1 \quad (1)$$

$$\frac{dA_2}{dt} = A_1 \times k_{12} - A_2 \times k_{21} \quad (2)$$

$$C_{\text{plasma}} = \frac{A_1}{V_1} \quad (3)$$

$$C_{\text{brain}} = f_u \times \frac{A_2}{V_2} \quad (4)$$

where A_1 and A_2 are the drug amounts in the central and brain compartments, respectively, t is time, k_{12} and k_{21} are the first-order distribution rate constants, V_M is the maximum enzymatic velocity, k_M is the MM constant, C_{plasma} is the observed plasma concentration, C_{brain} is the free concentration measured by μD in the brain, V_1 represents the volume of the central compartment, and V_2 is the volume of distribution in the peripheral compartment, respectively, considering only free drug concentrations measured in it ($f_u = 0.35$).

The estimated parameter values are presented in Table 1. All parameters were well estimated, with low relative standard errors (RSE).

Separate residual error models were used for total plasma concentrations and free brain concentrations. Based on goodness-of-fit plots and lower Akaike's information criterion (AIC), the best residual error model for the total plasma concentrations was the proportional model, while that for the free brain concentrations was the combined model.

The covariate body weight did not influence the model performance, but the categorical covariate infection showed a strong influence on V_2 ($P = 0.0017$, Wald test)

TABLE 1 Parameter estimates in the final VCZ population PK model[a]

Parameter	Estimate	RSE (%)	Interindividual variability	RSE (%)
$V_{1\ pop}$ (liters)	0.241	10		
$V_{2\_healthy}$ (liters)	0.352	12	0.258	21
$V_{2\_infected}$ (liters)	0.216	12	0.258	21
$\beta\_V2\_infected$	−0.487	32	NA	NA
$k_{12\ pop}$ (h^{-1})	8.530	22	0.458	21
$k_{21\ pop}$ (h^{-1})	6.130	8		
$V_{M\_healthy}$ (μg/ml)	0.324	13	0.312	21
$V_{M\_infected}$ (μg/ml)	0.186	15	0.312	21
$\beta\_VM\_infected$	−0.557	34	NA	NA
k_M (μg/ml)	0.540			
Residual variability				
Proportional, plasma	0.118	8	NA	NA
Combined, brain				
Additive	0.025	28	NA	NA
Proportional	0.041	27	NA	NA
Log-likelihood estimation				
AIC	−383.29	NA	NA	NA

[a]NA, not applicable; RSE, relative standard error (standard error of estimate/estimate × 100).

and V_M ($P = 0.0029$, Wald test), representing AIC reductions of 5.47 and 4.56 points, respectively. Equations 5 and 6 describe the linear covariate model:

$$V_{2\_infected} = V_{2\_healthy} \times e^{\beta\_V2\_infected} \quad (5)$$

$$V_{M\_infected} = V_{M\_healthy} \times e^{\beta\_VM\_infected} \quad (6)$$

where $V_{2\_healthy}$ is volume of distribution in the peripheral compartment in healthy animals, $V_{2\_infected}$ is volume of distribution in the peripheral compartment in infected animals, $V_{M\_healthy}$ is the maximum rate of metabolism in healthy animals, $V_{M\_infected}$ is the maximum rate of metabolism in infected animals, $\beta\_V_{2\_infected}$ is the exponential scaling factor for V_2, and $\beta\_V_{M\_infected}$ is the exponential scaling factor for V_M ($n = 12$).

For both total plasma and free brain concentrations, the predicted and observed concentrations are overall in good agreement (Fig. 2).

DISCUSSION

Considering that currently there are only two classes of systemic antifungal agents (polyenes and azoles) available for the treatment of fungal infections associated with *C. neoformans*, one strategy to improve the treatment in a fast, cheap, and safe way is to expand the use of existing drugs to another types of infections. An example of applying this strategy is the current indication of VRC as a new alternative drug for the treatment of infections associated with this yeast based on clinical observations. The doses indicated for the treatment are estimated empirically (4 to 7.5 mg/kg of body weight twice a day [b.i.d.]), and there are no studies that evaluated the drug's brain penetration during infection with this yeast (1, 4, 7).

Even for the drugs that are traditionally employed in the treatment of cryptococcal meningitis, such as amphotericin B and fluconazole, studies evaluating the influence of the infection on the drug's brain distribution are scarce. Wu et al. (26) investigated the influence of P-glycoprotein on the pharmacokinetics of amphotericin B in healthy and *C. neoformans*-infected mice. The brain/plasma ratios (brain data estimated from tissue homogenate) were 2.0 for healthy animals and 1.2 for infected animals, indicating that the infection reduced the drug distribution in the brain. In a recent study, our research group investigated fluconazole brain penetration in healthy and *C. neoformans*-infected rats by μD; the $AUC_{brain}/fAUC$ ratios were 0.69 and 1.04 for these groups, respectively, showing that the free interstitial levels of fluconazole were increased during infection (27). Until now there were no reports in the literature describing the VRC penetration

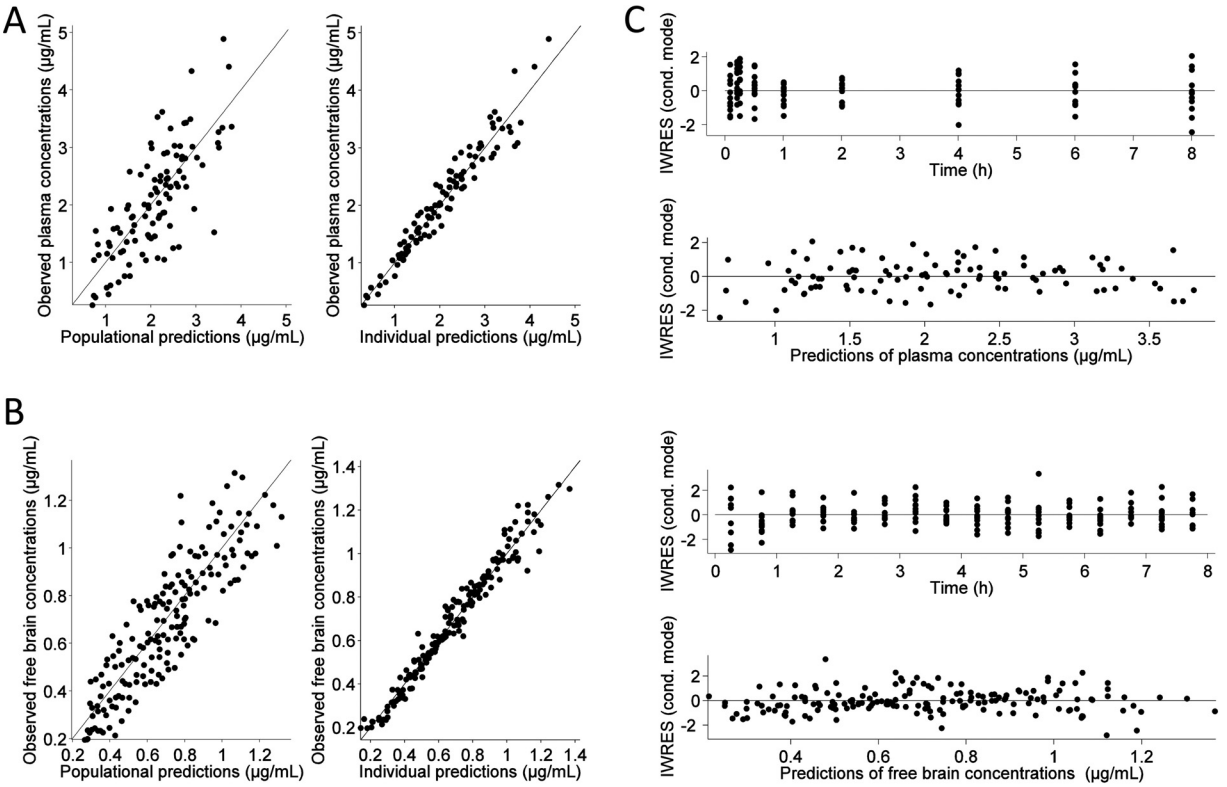

FIG 2 Goodness-of-fit plots for VCZ total plasma (A) and free brain (B) concentrations. In the plots of observations versus populational predictions and observations versus individual predictions, the gray line represents the linear regression fit and the black line is the identity line. In the graphs on the right (C), the residual plots are shown in which a black line is the LOESS smooth fit representing the trend in the data.

in the brain in healthy and *C. neoformans*-infected rats as determined by using the μD technique.

Lutsar et al. (28) investigated the VRC levels reached in the cerebrospinal fluid (CSF) during invasive fungal infections in patients; the CSF/plasma ratio was 0.59, indicating a reduced central nervous system (CNS) penetration of the drug in spite of the drug's characteristics that can aid its penetration in brain tissue, such as its moderated lipophilicity and large volume of distribution. *C. neoformans* is able to invade the brain, and the infection may extend from the meninges toward the cerebral parenchyma, producing small cysts with fungi inside (29); as a result, the concentrations reached in the interstitial space fluid are more representative of its effects.

In the present study, changes in the brain distribution of VRC during *C. neoformans* infection in rats were observed, and by using a two-compartmental with MM elimination, it was possible to demonstrate that the infection was able to change the pharmacokinetics parameters, such as volume of peripheral distribution (V_2) and maximum rate of metabolism (V_M) (23). Roffey et al. (30) and our group (25) had previously noted that at doses above 5 mg/kg, VRC exhibits nonlinear pharmacokinetics due to saturation of metabolism in healthy rats.

The enhancement of the drug's penetration and reduction on V_2 observed during the infection can be explaining by the pathogenesis of *C. neoformans* in the brain. Changes are reported in the microvascular environment (31) indicating modifications in the cytoskeleton and tight junctions in brain endothelial cells of the blood-brain barrier (32), and these events can improve the VRC permeability across the barrier. Another event related to the infection is the reduction in local pH (5.5) observed due to the presence of phagocytic cells. This phenomenon for basic drugs such as VRC (pK_a = 12.71) (2) produces the drug's ionization and may result in an ion-trapping effect. Given that VRC presents major elimination (98%) by the metabolic pathway, including isoen-

zymes CYP2C19, CYP3A4, and CYP2C9, liver injury could reduce its metabolism, reducing the value of V_M in infected animals (33–35).

In spite of the differences observed between VRC concentrations reached in healthy and infected tissues, the drug reached levels in both tissues higher than the MIC (range, 0.03 to 0.5 μg/ml) for *C. neoformans*, indicating the good drug potential for the treatment of cryptococcosis.

MATERIALS AND METHODS

Microorganisms. A strain of *Cryptococcus neoformans* var. *neoformans* (ATCC 28957) was employed in this study.

Animals. All experiments were approved by the Ethics in Research Committee of the Federal University of Rio Grande do Sul (protocol 26605). Wistar rats (weight, 150 to 350 g) were purchased from the Center of Reproduction and Experimental Animals Laboratory (CREAL). The rats were maintained under controlled temperature and humidity, with a 12-h light-dark cycle. Water and standard food were allowed *ad libitum* until the experiments were started.

System microdialysis. The μD system consisted of a PHD 2000 syringe pump (Harvard Apparatus, Holliston, MA). Gastight syringes (500 μl; Hamilton Company, Reno, NV) were used to provide the perfusate. CMA 12 probes for brain μD (3-mm polyarylethersulfone membrane and 20-kDa cutoff; CMA Microdialysis, Sweden) were used. Artificial cerebrospinal fluid (ACF; 145 mM NaCl, 2.7 mM KCl, 1.2 mM $CaCl_2$, 1 mM $MgCl_2$ [pH 7.4]) was used, prepared as described previously (36).

***In vitro* probe calibration.** Initially, *in vitro* NaCl μD experiments were carried out in order to investigate the influence of the flow rate and drug concentration on the relative recovery (RR) determined by dialysis (recovery) and retrodialysis (delivery) methods. The calibrations were determined at different flow rates (1.5, 2.0, and 2.5 μl/min) and concentrations (0.8, 0.5, and 0.35 μg/ml), and the experiments were performed as described by our research group previously (22).

The dialysis RR (RR_D) and retrodialysis recovery (RR_{RD}) were calculated according to equations 7 and 8:

$$\mathrm{RR_D}(\%) = \left(\frac{C_{\mathrm{dial}}}{C_{\mathrm{ext}}}\right) \times 100 \tag{7}$$

$$\mathrm{RR_D}(\%) = 100 - \left(\frac{C_{\mathrm{perf}} - C_{\mathrm{dial}}}{C_{\mathrm{perf}}} \times 100\right) \tag{8}$$

where C_{dial} is the VRC concentration in the microdialysate samples, C_{ext} is the VRC concentration in the medium surrounding the probe, and C_{perf} is the drug concentration in the perfusate solution.

***In vivo* probe calibration.** The calibrations were performed with healthy and infected male Wistar rats weighing 150 to 350 g (n = 3/group). VRC *in vivo* recovery was determined by retrodialysis using equation 8. The animals were anesthetized with a mixture of ketamine and xylazine (100 and 10 mg/kg, respectively), and after 1 h of equilibrium, a VRC concentration of 0.35 μg/ml in ACF was perfused at a flow rate of 2.0 ml/min.

Induction of infection. To prepare the standardized inoculum for a calibration curve, the protocol described by the CLSI (in CLSI document M27-A3 [37]) for antifungal susceptibility testing of yeasts was applied. Yeast suspensions from colonies grown for 72 h in 4% Sabouraud dextrose agar (SDA) at 37 $\pm$ 1°C were prepared in 0.9% sterile saline solution at different concentrations, and the transmittances of these suspension were read in a spectrophotometer (Analyser 800 M) at 530 nm. Suspensions were prepared in order to produce transmittances of 40, 50, and 60%. The experiment was performed in triplicate. After the transmittances were read, the yeast suspensions were successively diluted 10-fold, plated in 4% SDA, and incubated at 37 $\pm$ 1°C for 72 h, in duplicate. The total yeast count was determined for each transmittance level. A calibration curve was constructed by plotting the transmittance versus yeast cell count. The inoculum size chosen for the experiments (2.5×10^6 CFU/ml) corresponds to a transmittance of 50%. The disseminative infection was induced by injection of 100 μl of an inoculum of *C. neoformans* (1×10^6 CFU/ml) intravenously in the lateral tail vein. The infection was established 10 days postinoculation. The presence of *C. neoformans* in the brain was investigated by histological and microbiological assays (23).

Quantification of VRC in plasma and microdialysate samples. The quantification of VRC in rat plasma and microdialysate samples was performed by liquid chromatography with tandem mass spectrometry (LC-MS/MS) and liquid chromatography with UV detection (LC-UV), respectively, and both methods were validated according to FDA guidelines. The determination of VRC in microdialysate samples was conducted using a high-performance liquid chromatography (HPLC) method described by our group (22). A linear calibration curve was obtained in the range of 0.025 to 2.5 μg/ml using drug peak area and artificial cerebrospinal fluid as a matrix. VRC retention time was approximately 3.5 min. The microdialysate samples obtained were directly injected by the autosampler (30 μl) without previous preparation.

The plasma samples were quantified by LC-MS/MS for determination of VRC in rat plasma, using ketoconazole as the internal standard (IS) (38). The retention times of VRC and the IS were approximately 3.3 and 2.7 min, respectively. Calibration curves in spiked plasma were linear over a concentration range of 0.05 to 5.0 μg/ml, with a determination coefficient of $>$0.98. The lower limit of quantification was 0.05 μg/ml.

Pharmacokinetics protocols. (i) Surgical procedures. Blood and microdialysate sampling was performed through jugular vein cannulation and μD probe brain insertion, respectively. For blood sampling, a Silastic medical-grade tubing (Dow Corning, USA) was placed in the right jugular vein and

subcutaneously passed to the posterior surface of the neck, out of the reach of the animal. To avoid clotting, the catheter was filled with heparin solution (100 IU/ml in phosphate buffer; pH, 7.4 ± 0.1). After jugular vein cannulation surgery, the animal was positioned in a stereotaxic apparatus (ASI Instruments, USA) after being anesthetized with a mixture of ketamine and xylazine (100 and 10 mg/kg, respectively). A CMA 12 guide cannula was inserted into the primary motor cortex (according to the brain atlas of Paxinos and Watson in the following coordinates: 2.2 of anteriority, 2.8 of laterality, and 3.6 of posteriority) (39) and fixed with two screws and dental cement (Vip Flash, Brazil). The rats recovered from the surgery in individual polypropylene boxes for 48 h. One hour before the experiment, the animals were placed in a CMA 120 system for freely moving animals (CMA Microdialysis, Sweden) and the guide cannula was carefully replaced with a previously calibrated CMA 12 probe (3-mm polyarylethersulfone membrane and 20-kDa cutoff; CMA Microdialysis, Sweden) for brain μD.

(ii) VRC brain penetration experimental design. To determine VRC brain penetration, male Wistar rats were divided into a healthy group ($n = 7$) and an infected group ($n = 5$). All animals received VRC at 5 mg/kg by intravenous injection into the tail vein.

For both groups, the surgery to implant the probes and jugular cannula was done as described above and ACF solution was pumped at a flow rate of 2.0 μl/min. The microdialysate samples were harvested every 30 min (60 μl) and blood samples were taken at 0.08, 0.25, 0.5, 1, 2, 4, 6, and 8 h after VRC administration. The unbound VRC concentrations in the brain were determined by correcting the measured microdialysate concentrations by the $RR_{in\ vivo}$.

(iii) Determination of plasma protein binding. VRC protein binding was determined by ultrafiltration. The procedures used were the same previously described by our research group (40). To perform this step, plasma samples from healthy ($n = 3$) and *C. neoformans*-infected ($n = 3$) Wistar rats were used. Different VRC concentrations (0.075, 0.4, and 0.8 μg/ml) were investigated, based on the total plasma concentrations observed in the animals after intravenous administration of 5 mg/kg.

(iv) Pharmacokinetics analysis. The total area under the concentration-time curve from 0 h to infinity ($tAUC_{0-\infty}$) was calculated by linear trapezoidal rule for plasma and tissue data. VRC penetration into the brain (*f*T) was determined as the ratio between free tissue and free plasma ($tAUC_{0-\infty,tissue}/f_u \times tAUC_{0-\infty,plasma}$), where f_u is the unbound fraction in rat plasma. The *f*AUCs were compared by Student's *t* test ($\alpha = 0.05$) employing SigmaStat version 3.5 (Systat Software, Richmond, CA).

Population pharmacokinetic analysis (popPK) was performed using Monolix software version 4.3.3 (LIXOFT, Paris, France). A total of 290 observations (114 plasma and 176 brain measurements) derived from 12 rats (7 healthy and 5 infected) were included in the data set for the popPK analysis. Plasma and brain microdialysate samples were simultaneously fitted to the model.

The interindividual variability on fixed-effect model parameters was described equation 9 using an exponential model:

$$P_i = P_{\text{pop}} \times \exp(\eta_{i,p}) \quad (9)$$

where P_i represents the parameter estimate for the individual log-normally distributed, P_{pop} is the typical parameter estimate in the population, and $\eta_{i,P}$ is the random effect accounting for the individual difference from the typical value normally distributed with a mean of 0 and variance Ω. Correlations between random effects were tested. The residual variability was tested with additive, proportional, and combined error models.

The effect of continuous covariate body weight and the categorical variable infection by *C. neoformans* on PK parameters was investigated once an adequate model was finalized. The covariate term was selected using both a likelihood ratio test (LRT) and Wald test ($P < 0.05$), the improvement of the precision of the parameter estimates, and goodness-of-fit plots. The LRT was used for testing the significance of a covariate in the model using forward inclusion (LRT, $P < 0.05$) followed by backward elimination (LRT, $P < 0.01$). The goodness of fit was evaluated by plots of population predicted and individual predicted values versus observed measurements and by evaluating the residuals via graphical inspection of weighted residuals versus time and weighted residuals versus individual predictions. A visual predictive check (VPC) was used in which the model and its final parameter estimates were used to simulate 1,000 concentration-time profiles and overlay the respective mean and variance estimates with those of the original data to assess the predictive performance of the model. The final model was obtained by testing several structural models that were compared using Akaike's information criterion (AIC), precision of the parameter estimates, physiological meaningfulness of parameter estimates, visual assessment of goodness-of-fit plots, and VPCs.

ACKNOWLEDGMENT

We acknowledge CNPq-Brazil for financial support (project 449972/2014-3).

REFERENCES

1. Polvi EJ, Li X, O'Meara TR, Leach MD, Cowen LE. 2015. Opportunistic yeast pathogens: reservoirs, virulence mechanisms, and therapeutic strategies. Cell Mol Life Sci 72:2261–2287. https://doi.org/10.1007/s00018-015-1860-z.
2. Adams AIH, Morimoto LN, Meneghini LZ, Bergold AM. 2008. Treatment of invasive fungal infections: stability of voriconazole infusion solutions in PVC bags. Braz J Infect Dis 12:400–404. https://doi.org/10.1590/S1413-86702008000500011.
3. Pelletier R, Loranger L, Marcotte H, De Carolis E. 2002. Voriconazole and fluconazole susceptibility of *Candida* isolates. J Med Microbiol 51:479–483. https://doi.org/10.1099/0022-1317-51-6-479.
4. Kon AS, Grumach AS, Colombo AL, Oliveira Penalva AC, Wanke B, de Queiroz Telles F, Severo LC, Aranha LF, dos Santos Lazéra M, Ribeiro Resende M, do Amparo Salmito M, Shikanai-Yasuda MA, Moretti ML, Simão Ferreira M, Silva-Vergara ML, Procópio Andrade NM, Trabasso P, Pôncio Mendes R, Martinez R, Ponzio V. 2008. Consenso em criptoco-

cose—2008. Rev Soc Bras Med Trop 41:524–544. https://doi.org/10.1590/S0037-86822008000500022.
5. Flores VG, Tovar RMC, Zaldivar PG, Martinez EA. 2012. Meningitis due to *Cryptococcus neoformans*: treatment with posaconazole. Curr HIV Res 10:620–623. https://doi.org/10.2174/157016212803305970.
6. Girmenia C, Tuccinardi C, Santilli S, Mondello F, Monaco M, Cassone A, Martino P. 2000. In vitro activity of fluconazole and voriconazole against isolates of *Candida albicans* from patients with haematological malignancies. J Antimicrob Chemother 46:479–484. https://doi.org/10.1093/jac/46.3.479.
7. Yao Y, Zhang J-T, Yan B, Gao T, Xing X-W, Tian C-L, Huang X-S, Yu S-Y. 2015. Voriconazole: a novel treatment option for cryptococcal meningitis. Infect Dis (London) 47:694–700. https://doi.org/10.3109/23744235.2015.1044260.
8. Inoue A, Harada H, Iwata S, Teraoka M, Yamashita D, Kumon Y, Ohnishi T. 2012. Intraventricular cryptococcoma successfully treated with liposomal amphotericin B and voriconazole: a case report. No Shinkei Geka 40:777–784. (In Japanese.)
9. Ogaki K, Noda K, Fukae J, Furuya T, Hirayama T, Fujishima K, Hattori N, Okuma Y. 2010. Cryptococcal meningitis successfully treated with liposomal amphotericin B and voriconazole in an elderly patient. Brain Nerve 62:1337–1340. (In Japanese.)
10. Sabbatani S, Manfredi R, Pavoni M, Consales A, Chiodo F. 2004. Voriconazole proves effective in long-term treatment of a cerebral cryptococcoma in a chronic nephropathic HIV-negative patient, after fluconazole failure. Mycopathologia 158:165–171. https://doi.org/10.1023/B:MYCO.0000041904.71381.e3.
11. Como JA, Dismukes WE. 1994. Oral azole drugs as systemic antifungal therapy. N Engl J Med 330:263–272. https://doi.org/10.1056/NEJM199401273300407.
12. Capone D, Tarantino G, Gentile A, Sabbatini M, Polichetti G, Santangelo M, Nappi R, Ciotola A, D'Alessandro V, Renda A, Basile V, Federico S. 2010. Effects of voriconazole on tacrolimus metabolism in a kidney transplant recipient. J Clin Pharm Ther 35:121–124. https://doi.org/10.1111/j.1365-2710.2009.01070.x.
13. Lempers VJ, van den Heuvel JJ, Russel FG, Aarnoutse RE, Burger DM, Brüggemann RJ, Koenderink JB. 2016. Inhibitory potential of antifungal drugs on ATP-binding cassette transporters P-glycoprotein, MRP1 to MRP5, BCRP, and BSEP. Antimicrob Agents Chemother 60:3372–3379. https://doi.org/10.1128/AAC.02931-15.
14. Billaud EM. 2007. Interactions métaboliques des antifongiques azolés. J Mycol Med 17:168–176. https://doi.org/10.1016/j.mycmed.2007.05.004.
15. Felton T, Troke PF, Hope WW. 2014. Tissue penetration of antifungal agents. Clin Microbiol Rev 27:68–88. https://doi.org/10.1128/CMR.00046-13.
16. Paulzen M, Gründer G, Veselinovic T, Wolf B, Hiemke C, Lammertz SE. 2016. Duloxetine enters the brain—but why is it not found in the cerebrospinal fluid. J Affect Disord 189:159–163. https://doi.org/10.1016/j.jad.2015.08.073.
17. Hammarlund-Udenaes M, Fridén M, Syvänen S, Gupta A. 2008. On the rate and extent of drug delivery to the brain. Pharm Res 25:1737–1750. https://doi.org/10.1007/s11095-007-9502-2.
18. Joukhadar C, Derendorf H, Müller M. 2001. Microdialysis. A novel tool for clinical studies of anti-infective agents. Eur J Clin Pharmacol 57:211–219.
19. Zimmermann ES, Torres BGS, Dalla Costa T. 2016. Validation of a sensitive HPLC/fluorescence method for assessment of ciprofloxacin levels in plasma and prostate microdialysate samples from rats. Biomed Chromatogr 30:330–336.
20. Hurtado FK, Weber B, Derendorf H, Hochhaus G, Dalla Costa T. 2014. Population pharmacokinetic modeling of the unbound levofloxacin concentrations in rat plasma and prostate tissue measured by microdialysis. Antimicrob Agents Chemother 58:678–686. https://doi.org/10.1128/AAC.01884-13.
21. Romani L, Bistoni F, Puccetti P. 2003. Adaptation of *Candida albicans* to the host environment: the role of morphogenesis in virulence and survival in mammalian hosts. Curr Opin Microbiol 6:338–343. https://doi.org/10.1016/S1369-5274(03)00081-X.
22. de Araujo BV, da Silva CF, Haas SE, Costa TD. 2009. Free renal levels of voriconazole determined by microdialysis in healthy and Candida sp.-infected Wistar rats. Int J Antimicrob Agents 33:154–159. https://doi.org/10.1016/j.ijantimicag.2008.08.020.
23. Staudt KJ, Colombo GA, Alves IA, Araújo BV. 2016. Disseminative infection model by *Cryptococcus neoformans* in male Wistar rats. p 58. Abstr III ABCF Congr. Brazilian Association of Pharmaceutical Sciences, Porto Alegre, Brazil.
24. Azeredo FJ, Hass SE, Sansone P, Derendorf H, Costa TD, De Araujo BV. 2015. Does the anesthetic urethane influence the pharmacokinetics of antifungal drugs? A population pharmacokinetic investigation in rats. J Pharm Sci 104:3314–3318.
25. Araujo BV, Farias da Silva C, Costa TD. 2010. An alternative approach to determine oral bioavailability of drugs that follow Michaelis-Menten elimination: a case study with voriconazole. Pharmacology 86:163–167. https://doi.org/10.1159/000317066.
26. Wu J-Q, Shao K, Wang X, Wang R-Y, Cao Y-H, Yu Y-Q, Lou J-N, Chen Y-Q, Zhao H-Z, Zhang Q-Q, Weng X-H, Jiang C, Zhu L-P. 2014. In vitro and in vivo evidence for amphotericin B as a P-glycoprotein substrate on the blood-brain barrier. Antimicrob Agents Chemother 58:4464–4469. https://doi.org/10.1128/AAC.02535-14.
27. Alves IA, Lock GA, Rates SM, Araujo BV. 2016. Impact of meningitis caused by *Cryptococcus neoformans* in Wistar rats in azole's penetration in the brain, p 359. Abstr III ABCF Congr. Brazilian Association of Pharmaceutical Sciences, Porto Alegre, Brazil.
28. Lutsar I, Roffey S, Troke P. 2003. Voriconazole concentrations in the cerebrospinal fluid and brain tissue of guinea pigs and immunocompromised patients. Clin Infect Dis 37:728–732. https://doi.org/10.1086/377131.
29. Fobe JL, De Buone ML, Da Costa RB. 1995. Cryptococcal granuloma of the brain: case report. Arq Neuropsiquiatr 53:802–806.
30. Roffey SJ, Cole S, Comby P, Gibson D, Jezequel SG, Nedderman ANR, Smith DA, Walker DK, Wood N. 2003. The disposition of voriconazole in mouse, rat, rabbit, guinea pig, dog, and human. Drug Metab Dispos Biol Fate Chem 31:731–741. https://doi.org/10.1124/dmd.31.6.731.
31. Chang YC, Stins MF, McCaffery MJ, Miller GF, Pare DR, Dam T, Paul-Satyaseela M, Kim KS, Kwon-Chung KJ, Paul-Satyasee M. 2004. Cryptococcal yeast cells invade the central nervous system via transcellular penetration of the blood-brain barrier. Infect Immun 72:4985–4995. https://doi.org/10.1128/IAI.72.9.4985-4995.2004.
32. Chen SHM, Stins MF, Huang S-H, Chen YH, Kwon-Chung KJ, Chang Y, Kim KS, Suzuki K, Jong AY. 2003. *Cryptococcus neoformans* induces alterations in the cytoskeleton of human brain microvascular endothelial cells. J Med Microbiol 52:961–970. https://doi.org/10.1099/jmm.0.05230-0.
33. Dote S, Sawai M, Nozaki A, Naruhashi K, Kobayashi Y, Nakanishi H. 2016. A retrospective analysis of patient-specific factors on voriconazole clearance. J Pharm Health Care Sci 2:10. https://doi.org/10.1186/s40780-016-0044-9.
34. Hohmann N, Kocheise F, Carls A, Burhenne J, Weiss J, Haefeli WE, Mikus G. 2016. Dose-dependent bioavailability and CYP3A inhibition contribute to non-linear pharmacokinetics of voriconazole. Clin Pharmacokinet 55:1535–1545. https://doi.org/10.1007/s40262-016-0416-1.
35. Li X, Yu C, Wang T, Chen K, Zhai S, Tang H. 2016. Effect of cytochrome P450 2C19 polymorphisms on the clinical outcomes of voriconazole: a systematic review and meta-analysis. Eur J Clin Pharmacol 72:1185–1193. https://doi.org/10.1007/s00228-016-2089-y.
36. Carreño F, Paese K, Silva CM, Guterres SS, Dalla Costa T. 2016. Pharmacokinetic investigation of quetiapine transport across blood-brain barrier mediated by lipid core nanocapsules using brain microdialysis in rats. Mol Pharm 13:1289–1297. https://doi.org/10.1021/acs.molpharmaceut.5b00875.
37. CLSI. 2008. Reference method for broth dilution antifungal susceptibility testing of yeasts; approved standard, 3rd ed. CLSI document M27-A3. CLSI, Wayne, PA.
38. Araujo BV, Conrado DJ, Palma EC, Dalla Costa T. 2007. Validation of rapid and simple LC-MS/MS method for determination of voriconazole in rat plasma. J Pharm Biomed Anal 44:985–990. https://doi.org/10.1016/j.jpba.2007.03.026.
39. Paxinos G, Watson C. 2006. The rat brain in stereotaxic coordinates. Academic Press, New York, NY.
40. Torres BGS, Uchôa FDT, Canto RFS, Crestani A, Eifler-Lima V, Costa TD. 2014. Bioanalytical method for the quantification of the monastrol derivative anticancer candidate lasom 65 in pre-clinical pharmacokinetic investigations. Quim Nova 37:461–464. https://doi.org/10.5935/0100-4042.20140082.